Topological and chiral superconductor nanoarchitectures

Rosa Córdoba[1,*] and Vladimir M. Fomin[2,3,†]

[1]*Institute of Molecular Science (ICMol), Universitat de València, C/ Catedrático José Beltrán, 2, 46980 Paterna, València, Spain*
[2]*Institute for Emerging Electronic Technologies, Leibniz IFW Dresden, Helmholtzstraße 20, 01069 Dresden, Germany*
[3]*Faculty of Physics and Engineering, Moldova State University, Str. A. Mateevici 60, 2009 Chişinău, Republic of Moldova*

3D nano-superconductors, with non-trivial geometry-driven topological phenomena, stand as promising systems for the future evolution of efficient and multifunctional technologies. However, the substantial challenges inherent in the experimental work, particularly regarding the fabrication and characterization of 3D nanoscale geometries and unconventional topologies of superconducting states, have confined the majority of investigations in this domain until recently to the realms of computational and theoretical studies. We overview the recent advancements in fabricating superconductor 3D nanoarchitectures and unveiling their fascinating physical properties that occur due to the geometry-induced topology and chirality, which offer a broad spectrum of applications of these nanostructures for the front-line development of various modern technologies.

I. INTRODUCTION

The present letter is devoted to the revolutionizing penetration of two mathematical concepts in physics: "topology", which embraces the properties of a geometric object that are preserved under continuous deformations [1], and "chirality" that identifies the property of asymmetry of a system, which is distinguishable from its mirror image [2]. The both concepts have led to unprecedented wealth of results in physics. The realm of topological matter can be conventionally subdivided into two categories [3]. First, topologically protected surface/edge states governed by Dirac physics and/or topologically non-trivial electronic structure in the momentum space underlie the origin of quantum Hall effect, quantum spin Hall effect, quantum anomalous Hall effect, nonmagnetic topological insulators, topological crystalline insulators, topological semimetals [4] as well as topological superconductors and Majorana fermions. Second, non-trivial topology occurs due to a complex geometry of structures or fields in real space, e.g., quantum rings, Möbius bands [5], metamaterials of interlocked hollow semiconducting tori, optical waveguides, arrays of Josephson junctions, Skyrmions and other topologically non-trivial spin and magnetic textures [6]. Here an overview is provided of topology- and chirality-driven effects in the complex man-made geometries in real space, implemented by the recently developed high-tech methods to fabricate superconductor three-dimensional (3D) micro- and nanoarchitectures.

The incorporation of the third dimension into nano-superconductivity enables the deliberate manipulation of topology and chirality through the formulation of curved geometries. As a result, the integration of nanoscale dimensions with three-dimensional and curvilinear structures for the development of 3D nano-superconductors constitutes a noteworthy frontier in emerging physics [3,7].

It has been *theoretically predicted* that superconducting properties on 3D micro-superconductors, such as spherical shells [8], curved mesoscopic strips [9], hollow cylinders [10], thin-walled open cylinders [11,12], helices [13], and Möbius strips [14] are cardinally different from those observed in analogous 2D structures. Particularly, the Josephson effect can be regulated, with control over both the amplitude and phase of the supercurrent, and the confinement-induced curvature effects through the curved geometry of superconductors [15]. In addition, the distinctive vortex dynamics identified in curved geometries with particular topologies have been recognized as one of the most promising areas for research [16].

Experimental evidence, when conducted, has predominantly been confined to rudimentary 3D nano-superconductors or, in some instances, to 3D micro-superconductors that incompletely elucidate the boundless potential offered by a transition of nano-geometries into three dimensions.

In the subsequent two sections, we will firstly delineate the advancements achieved in fabricating genuine superconductor 3D nanoarchitectures. Secondly, we will expound upon the innovative properties experienced by these 3D nanoarchitectures induced by curved nano-geometries.

II. FABRICATION OF TOPOLOGICAL AND CHIRAL SUPERCONDUCTOR NANOARCHITECTURES

Experimental evidence has demonstrated that the pathways for fabricating complex SC 3D nanoarchitectures rely on sophisticated methodologies:

1) The utilization of *chemical synthesis* based on solid-gas reactions, notably evident in the fabrication of Transition Metal Dichalcogenide nanotubes, particularly WS_2 [17].

2) The employment of *free-standing superconducting rolled-up technology* [18,19], which allowed for fabrication of the first superconductor niobium radial superlattices [20,21] and which seamlessly integrates the 2D superconducting layer with a helical spiral curvature, as exemplified in the fabrication of microwave radiation detectors [22].

3) The adoption of *the conventional Dolan bridge technique* for the nanofabrication of 3D superconducting circuit suspended from the substrate [23]. This ground-breaking tech-

* Author to whom correspondence should be addressed: rosa.cordoba@uv.es
† Author to whom correspondence should be addressed: v.fomin@ifw-dresden.de

nique has facilitated the introduction of the elusive Blochnium superconducting qubit [24].

4) The utilization of a methodology based on *DNA self-assembly* to create 3D arrays of Josephson junctions, yielding niobium cubic superlattices with a 48 nm unit cell [25].

5) The strategic deployment of *3D nanoprinting techniques* to grow 3D nano-superconductors in a single step [26,27]. This approach has been used in fabricating wires [28–32], hollow nanocylinders [33,34] and nanohelices [35].

Several representative 3D superconductor nanoarchitectures are depicted in Fig. 1.

3D nanoprinting techniques rely on focused beams of charged particles, including ions, to form Focused Ion Beam (FIB), effectively address the significant limitations associated with traditional "top-bottom" nanofabrication methods in the development of 3D nano-superconductors [36]. The noteworthy advantage of 3D nanoprinting, in contrast to direct competitors like two-photon lithography [37] and electrodeposition [38], lies in its exceptionally high resolution (down to a few tens of nanometers [33–35]) and the ability to create shapes of arbitrary complexity [39]. Ga^+ FIB induced deposition (FIBID) (probe size $\approx$ 5 nm) has already been used to grow individual superconducting 3D W-C [28–30,32] and Nb-C [31] wires with T_c and B_{c2} similar to those obtained for planar nanostructures. However, the resolution in this process is primarily constrained by the Ga^+ beam diameter and its high lateral scattering, thus far preventing the growth of sub-100 nm 3D structures.

He^+ FIBID has demonstrated its significance in the development of 3D superconducting nanostructures characterized by intricate geometries, higher aspect ratios, and exceptional superconducting properties ($T_c \approx 6.2$ to 7.1 K, $B_{c2}(0) \approx 12$ to 15 T), exemplified by structures like hollow nanocylinders [33,34] and nanohelices [35]. This success is attributed to its diminutive probe size ($\approx$ 0.3 nm) [40] and minimal proximity effect [41]. Thus, He^+ FIBID marks a substantial leap forward in the direct-writing of 3D nano-objects when juxtaposed with Ga^+ FIBID.

An illustrative demonstration of these capabilities lies in the production of tailored 3D hollow nanocylinders, featuring diameters as small as 32 nm, wall thicknesses down to 13 nm, and an aspect ratio $\approx$ 200 [33,34]. The presence of a 6 nm diameter hole at the center of the standing cylinder results from a delicate balance between milling and deposition processes. The resulting material exhibits a higher tungsten content (reaching up to 70 atomic %) compared to that achieved through Ga^+ FIBID. Moreover, the presence of 20 to 30 nm-sized crystalline grains of the face-centered cubic WC_{1-x} phase is noted.

Another remarkable example involves the precise patterning of 3D nanohelices, achieved through meticulous adjustment of key deposition parameters such as dwell time and pattern diameter [35]. The geometry of the nanohelices is effectively controlled, with turn lengths ranging from 200 nm to 2.3 μm, nanohelix diameters spanning from 100 nm to 295 nm, and nanowire diameter as small as 45 nm. Notably, the fabrication of the smallest and most densely packed superconducting nanohelix to date is reported, measuring as tiny as 100 nm in diameter and exhibiting an impresive aspect ratio of 65. These nanohelices demonstrate superconductivity below 7 K, along with high upper critical magnetic fields $\mu_0 H_{c2} \approx 15$ T, and large critical current densities $J_c \approx 0.2$ MA/cm^2. To date, acquiring experimental evidence for 3D nano-superconductors through focused electron beam induced deposition (FEBID) has proven elusive, although the technique holds the potential to achieve this in the near future. Only a few studies have been reported, focusing on planar W-C [42,43] ($T_c \approx 2$ to 4.5 K), Pb-C [44] ($T_c \approx 7.3$ K) and Mo-C [45] ($T_c \approx 10$ K) FEBID superconducting materials using $W(CO)_6$, $(CH_3CH_2)_4Pb$ and $Mo(CO)_6$ as precursors, respectively. However, it is noteworthy that, at present, only simple 3D nano-superconductors have been created through trial and error methodologies. The fabrication of complex 3D superconductor nanoarchitectures remains elusive, as the current repertoire of patterning tools in FIB [46] and FEB [47–49] necessitates further exploration of available precursors that could enable the production of more sophisticated 3D nano-superconductors.

III. FASCINATING GEOMETRY-DRIVEN TOPOLOGICAL PHENOMENA DETERMINE PHYSICAL PROPERTIES OF 3D SUPERCONDUCTOR NANOARCHITECTURES

A. Experimental evidence

Fig. 2 illustrates various experimental instances showcasing geometry-induced topological phenomena in 3D superconductor nanoarchitectures.

Superconductivity in chiral nanotubes. Chiral WS_2 nanotubes reveal non-identical current behaviours under paraxial magnetic fields due to chirality [17]. Nonreciprocal superconducting transport, detected through second harmonic signals in AC magnetoresistance, reveals a chirality-induced effect on superconductivity. The nonreciprocal signals are notably enhanced in the superconducting state, featuring oscillations with a period equal to the magnetic flux quantum and increased magnitude around T_c, indicating quantum interference of the superconducting current. These chiral WS_2 nanotubes hold promise for superconductivity modulation via nonreciprocity (Fig. 2(a)).

Hollow nanocylinders [33,34] display superconducting characteristics below the critical temperature of $T_c = 6.3$ K, accompanied by a substantial critical magnetic field $\mu_0 H_{c2}(0) \approx$ 13.9 T and critical current density $J_c \approx 0.23$ MA/cm, which exceeds by 1.5 times the value for planar nanowires of comparable dimensions fabricated using Ga^+ FIBID. Below the critical value $B^* = 2.6$ T (defined as, the field, at which $J_c(B)$ is $0.9 J_c$ at 0 T), the behavior of J_c is influenced by the strong confinement potential of a single row of vortices at the core of the hollow nanocylinder [50] (Fig. 2(b)).

In a *rolled-up nanohelix*, the low-dimensionality of the superconducting niobium layer is combined with a helical spiral curvature in a transition-edge sensor [22]. The standalone sensor features an exceptionally low heat capacity and achieves an ultrafast response time. The supporting bilayer of the nanohelix is 50 nm, and the chiral geometry dictates minimal contact

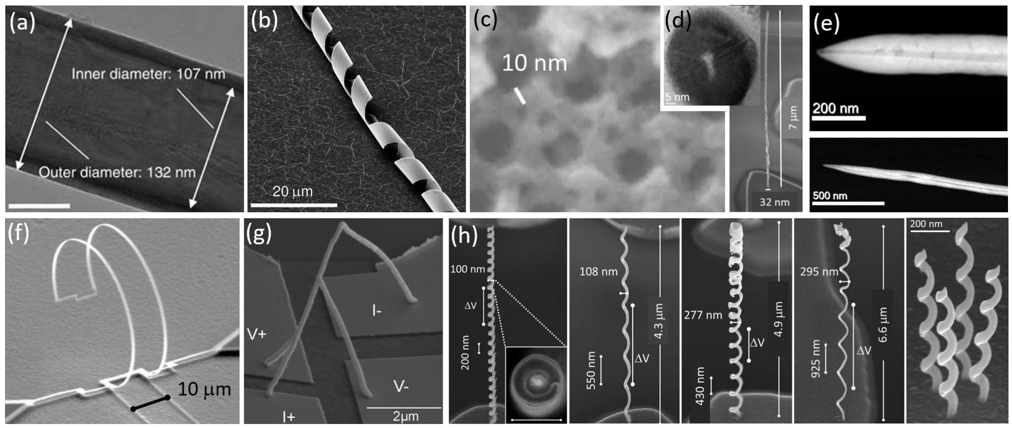

FIG. 1. Examples of 3D superconductor nanoarchitectures. (a) TEM image of a chemically synthesized chiral superconducting WS_2 nanotube. Contrast image shows the cylindrical structure with a diameter of about 100 nm. Scale bar, 50 nm. Reproduced with permission [17]. Copyright 2017, Springer Nature. (b) SEM image of a rolled-up Nb nanohelix. Reproduced with permission [22]. Copyright 2019, American Chemical Society. (c) SEM image 3D superconducting superlattices (with simple cubic symmetry and 48 nm unit cell) using self-assembly of 3D DNA frames. Adapted with permission [25]. Copyright 2020, Springer Nature. (d) SEM image of a hollow nanocylinder with outer diameter down to 32 nm grown using He^+ FIBID as a 3D nanoprinting technique. Inset: TEM image of the cross sectional view of the hollow nanocylinder with inner diameter down to 6 nm. Adapted with permission [33]. Copyright 2018, American Chemical Society. (e) STEM images of hollow nanocylinders with different inner and outer diameters grown using He^+ FIBID. Adapted with permission [34]. Copyright 2020 Beilstein-Institut. (f) SEM image of a fabricated Blochnium device using Dolan bridge technique. Adapted with permission [24]. Copyright 2020, Springer Nature. (g) SEM image of a freestanding 3D nanowire of width 170 nm grown using Ga^+ FIBID as a 3D nanoprinting technique. Reproduced with permission [31]. Copyright 2019, American Chemical Society. (h) SEM images of individual WC nanohelices with nanowire diameter of 45 nm and a nanohelices array grown using He^+ FIBID. ΔV represents the locations of the voltage contacts. Inset: the top view of the nanohelix. Scale bar: 100 nm. Adapted with permission [35]. Copyright 2019, American Chemical Society.

points between the transition-edge sensor and the substrate.

The *Blochnium superconducting qubit* exploits the coherent insulating response of a single Josephson Junction, resulting from the extension of phase fluctuations beyond 2π (Fig. 2(c)). A significant technological advancement of this research involves integrating a weak junction shunted with an exceptionally high inductance in a 3D superconducting circuit [24]. The radiofrequency excitation spectrum is analyzed while manipulating the external magnetic flux passing through the 3D loop, aligning with a duality mapping of Blochnium onto a transmon, which substitutes the external flux with the offset charge and introduces an alternative collective quasicharge variable.

The *DNA-based self-assembly* facilitates the formation of precisely organized 3D arrays of Josephson Junctions (Fig. 2(d)). Each pair of superconducting octahedra is intricately connected by a weak link, surpassing the niobium superconducting coherence length of approximately 40 nm. The low-temperature I–V curves of the array exhibit behaviour similar to that of an individual Josephson Junction [25].

Nanohelices. An enhancement of the magnetic field values (35 % larger compared to hollow nanocylinders [33]), at which the resistance reaches 10 % of its normal-state value, is observed for a nanohelix of a specific type [35]. Additionally, tilting the magnetic field reveals a significant influence on the upper critical magnetic field. At the same time, a nanohelix of a different type reveals characteristic features of vortex- and phase-slip-regimes, experimentally discerned through resistance steps in the I–V curves. These patterns are attributed to topologically non-trivial screening currents and confinement potentials in the helical 3D geometry. The experimental observations are supported by numerical simulations based on the time-dependent Ginzburg-Landau equation coupled with the Poisson equation. Simulations unveil various patterns of the order parameter corresponding to the spatial distribution of the normal-to-the-surface component of the magnetic field over the surface of the nanohelix at different values of the transport current (Fig. 2(e)).

B. Computational and theoretical studies

Dynamic topological transitions. Dynamic geometry-driven topological transitions in open superconductor nanotubes occur under a combined dc+ac transport current [51]. The key effect is a transition between two regimes of superconducting dynamics (Fig. 3(a)). The first regime is characterized by a pronounced first harmonic in the FFT spectrum

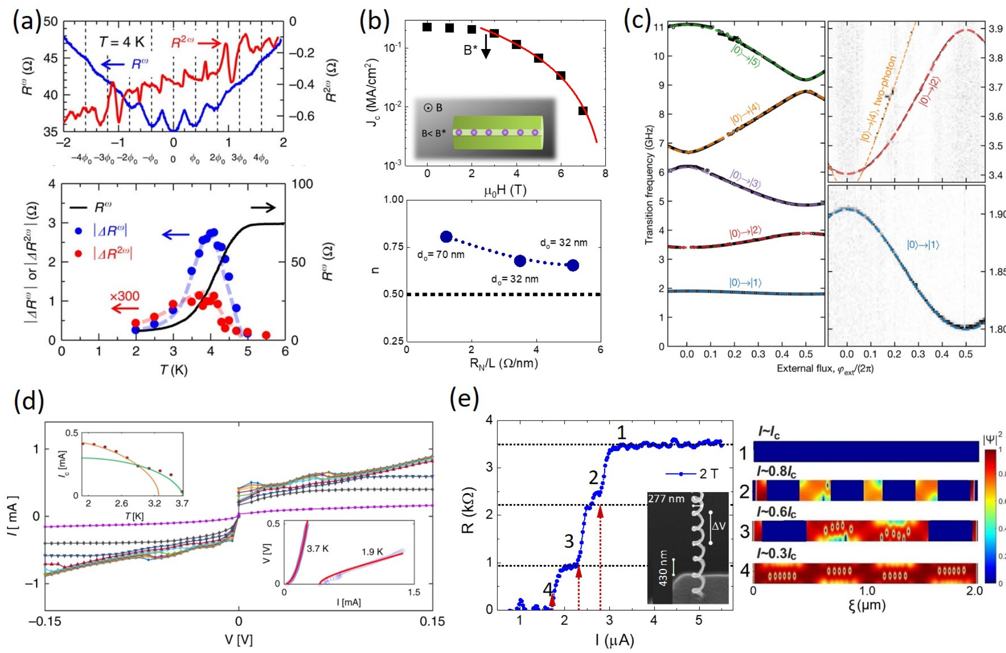

FIG. 2. Examples of geometry-driven topological phenomena of 3D superconductor nanoarchitectures. (a) Superconductor chiral nanotube (shown in Fig. 1(a). The upper panel displays a plot of R^{ω} and $R^{2\omega}$ in the low-magnetic field region at $T = 4$ K. Periodic oscillations are observed for both signals in the superconducting state. In the lower panel, the temperature variation of the resistance and magnitude of the quantum oscillations in R^{ω} and $R^{2\omega}$ is depicted. Both oscillating signals are enhanced around T_c. Reproduced with permission [17]. Copyright 2017, Springer Nature. (b) Hollow nanocylinders grown using He$^+$ FIBID. The upper panel shows the J_c as a function of the applied magnetic field at 0.5 K for a hollow nanocylinder with an outer diameter of 32 nm. The behavior of J_c below the critical value B^* (where $B^* = 2.63$ T, representing the field at which J_c is $0.9J_c$ at 0 T) is influenced by the strong confinement potential of a single row of vortices at the core of the hollow nanocylinder. Whereas for B above B^*, J_c is subjected to fitting using a potential equation indicative of collective vortex pinning. An inset illustration depicts the penetration of magnetic flux into the hollow nanocylinder, with a single vortex row forming at $B<B^*$. In the lower panel illustrates the dependence of n values on R_N/L for three nanocylinders. This dependency strongly indicates that smallest nanocylinders are approaching quasi-one-dimensional superconducting behavior. Adapted with permission [33]. Copyright 2019, American Chemical Society. (c) The Blochnium superconducting qubit (shown in Fig. 1(f)). In the left panel, transition frequencies extracted from the two-tone spectroscopy data are presented as a function of the external flux through the loop, along with the fit to the spectrum. The right panel displays a zoomed-in view of the raw data. Adapted with permission [24]. Copyright 2020, Springer Nature. (d) 3D arrays of Josephson junctions (shown in Fig. 1(c). The I–V characteristics were measured over the temperature range of 1.9–3.7 K. In the right inset, the V–I characteristics at 1.9 and 3.7 K are shown. In the left inset, the critical current derived from the I–V curves is presented as a function of temperature. Reproduced with permission [25]. Copyright 2020, Springer Nature. (e) Nanohelices. R–I characteristic is presented in the left panel for a nanohelix, while simulated order parameter distributions are depicted over the 2D surface of the helical structure in the right panel for magnetic field of 2 T. Various vortex and phase-slip patterns are associated with steps of resistance, as indicated by the red arrows. Inset: the tilted view of the nanohelix. Adapted with permission [35]. Copyright 2019, American Chemical Society.

of the induced voltage at the ac frequency. The second regime is represented by a rich FFT spectrum of the induced voltage with pronounced low-frequency components. The unveiled transitions between vortex- and phase-slip-based transport regimes in 3D nanoarchitectures governed by the global superconducting screening currents flowing over the entire structures are of topological nature and therefore are robust with respect to defects and impurities.

Deduction of vortex configurations from global observables. Various vortex chains, vortex jets, phase-slip regimes [52] occur in superconductor open nanotubes due to the inhomogeneity of the normal magnetic induction component $B_{\rm n}$ [11], which determines the topology of screening currents [53,54]. Traversing of the half-tubes by dc-driven vortices induces GHz-frequency voltage U oscillations with spectrum $f_{\rm U}(B)$ (Fig. 3(b)). Integer harmonics nf_1 (f_1 is the vortex nucleation frequency, $n \geq 2$) correspond to a single vortex-chain regime at low B. At higher fields, non-integer harmonics $\frac{n}{m} f_1$ ($m \geq 2, m \neq n$) are indicative of the presence of m chains in the vortex jets. Peaks in dU/dB and jumps in the frequency of microwave generation occur when the number of fluxons moving in the half-tubes increases by one. Thus, vortex jets can be efficiently constrained and steered using the curvature of 3D superconductor membranes.

Steering of vortices by magnetic-field tiltings Steering of vortex chains and jets in superconductor open nanotubes [55] is provided by tilting of the magnetic field $\mathbf{B}$ at an angle α in the plane perpendicular to the axis of a nanotube carrying an azimuthal transport current. An increase of α displaces the areas with the close-to-maximum normal component $|B_n|$ to the close(opposite)-to-slit regions. At lower B, close-to-slit vortex chains disappear, yielding $f_U(B)$ consisting of integer harmonics nf_1. At higher B, $f_f(U)$ is largely blurry because of multifurcations of vortex trajectories, giving rise to coexistence of a vortex jet with two vortex chains at $\alpha = 90°$. This behavior is explained by the analysis of the modulus of the order parameter $|\psi(x,y)|$ as a function of α and B overlaid with the accumulated vortex trajectories (Fig. 3(c)).

IV. PERSPECTIVES OF TOPOLOGICAL AND CHIRAL NANOARCHITECTURES FOR APPLICATIONS OF SUPERCONDUCTOR MATERIALS

Sensitive superconducting bolometers. In [22], a significant improvement of the microwave radiation detection has been demonstrated through the fabrication of a superconducting bolometer by self-rolling 2D superconductor structures into 3D helical belts. The sensitivity measurements (Fig. 4(a)) revealed that the nanohelix features a noise equivalent power (NEP) of $\sim 2\times 10^{10}$ WHz$^{1/2}$ at a microwave radiation power of 9 Wm^{-2}, which is 4 orders of magnitude smaller than the NEP of the commercially available QMC sensor at a similar radiation power. The reason is the extremely low heat capacity of the 50 nm thick supporting material and the few contact points between the transition-edge-sensor and the substrate.

Superconducting memory elements. A miniaturized superconducting memory cell employing a 3D Nb nano-SQUID is presented, featuring tunable hysteresis between flux quantum states [56]. The measured current-phase relations of nano-SQUIDs exhibit skewness correlated with critical current and hysteresis loop size. This skewed relations enables further memory cell miniaturization by overcoming loop inductance limitations, advancing superconducting memory technology.

Superconducting thermoelectric elements. Including a curved 3D geometry enhances performance of superconducting tunnel junctions, which exhibit significant bipolar thermoelectricity under thermal gradients due to particle–hole symmetry breaking. Integrated into Josephson interferometers, they could act as bipolar thermoelectric Josephson engines [57].

Superconducting quantum circuits. Exploring macroscopic quantum dynamics in ultrahigh-impedance circuits is suggested for application in quantum computing and metrology. The Blochnium qubit utilizes hyperinductance ($L \approx 2.5\,\mu$H, $\omega/2\pi > 13$ GHz, $L\omega > 200k\Omega$), enabling fault-tolerant operations on superconducting qubits [24].

Electric field-induced control of superconductivity. An initiative involves integrating advanced superconductors into 3D Field-Effect Transistors [58] to control the superconducting transition as well as vortex and phase slip dynamics using an electric field [59]. The 3D geometry aims to mitigate challenges from planar structures [60], enhancing electrical characteristics and addressing reliability concerns (Fig. 4(b)).

High-sensitivity magnetic-field sensors. Nanosystems are perspective as building blocks for constructing 3D Josephson Junctions, aiming to control phase slip events for reversible decoherence in Josephson weak links using an electric field [61]. These components could offer high stability and operational robustness, serving various applications, such as scanning probe microscopy tips and sensitive SQUID-on-tip (SOT) devices [62,63]. Imaging of superconducting vortices in amorphous MoSi thin films with a SOT sensor was demonstrated [64]. Functioning at low temperatures and under high magnetic fields, these sensors could serve as ideal probes for electron spin sensing and vortex imaging in superconductors.

Single-photon detectors. Ultra-fast vortex motion is demonstrated in Nb-C microwires grown with Ga^+ FIBID [65], presenting an opportunity to study non-equilibrium superconducting systems (Fig. 4(c)). Incorporating a curved 3D geometry is expected to enhance their weak vortex pinning, critical currents near the depairing current, and rapid heat dissipation from heated electrons, making them promising candidates for fast single-photon detectors.

V. VISIONARY OUTLOOK: CHALLENGES AND WAYS TO ADDRESS THEM

A. in the experimental work

To fully harness the potential of transition into three dimensions, addressing substantial experimental challenges related to the fabrication and characterization of intricate 3D nanoscale geometries and topological configurations is imperative [66,67].

i) Advanced nanofabrication methods: a self-spooling of $NbSe_3$ Möbius-stripes and other architectures on spontaneously emerging Se balls[68]; a physical vapor deposition technique called Glancing Angle Deposition (GLAD) [69]; 3D roll-up self-organization [18,19,22]; direct-writing techniques using FEBID; automated design of 3D DNA-based origami with non-rasterized 2D curvature [70]. To obtain reproducible results, precise control over experimental conditions is required ensuring consistent production of superconductor 3D nanoarchitectures with desired physical and chemical properties.

ii) Advanced characterization methodology: The characterization of 3D curved superconductors at the nanoscale has, thus far, been constrained to a limited set of experimental techniques, as detailed in Section II of the current article. These include electrical magnetotransport measurements (Fig. 2(a), 2(b), 2(d), 2(e) and Fig. 4(b) and Fig. 4(c), two-tone radiofrequency spectroscopy Fig. 2(f), and microwave radiation de-

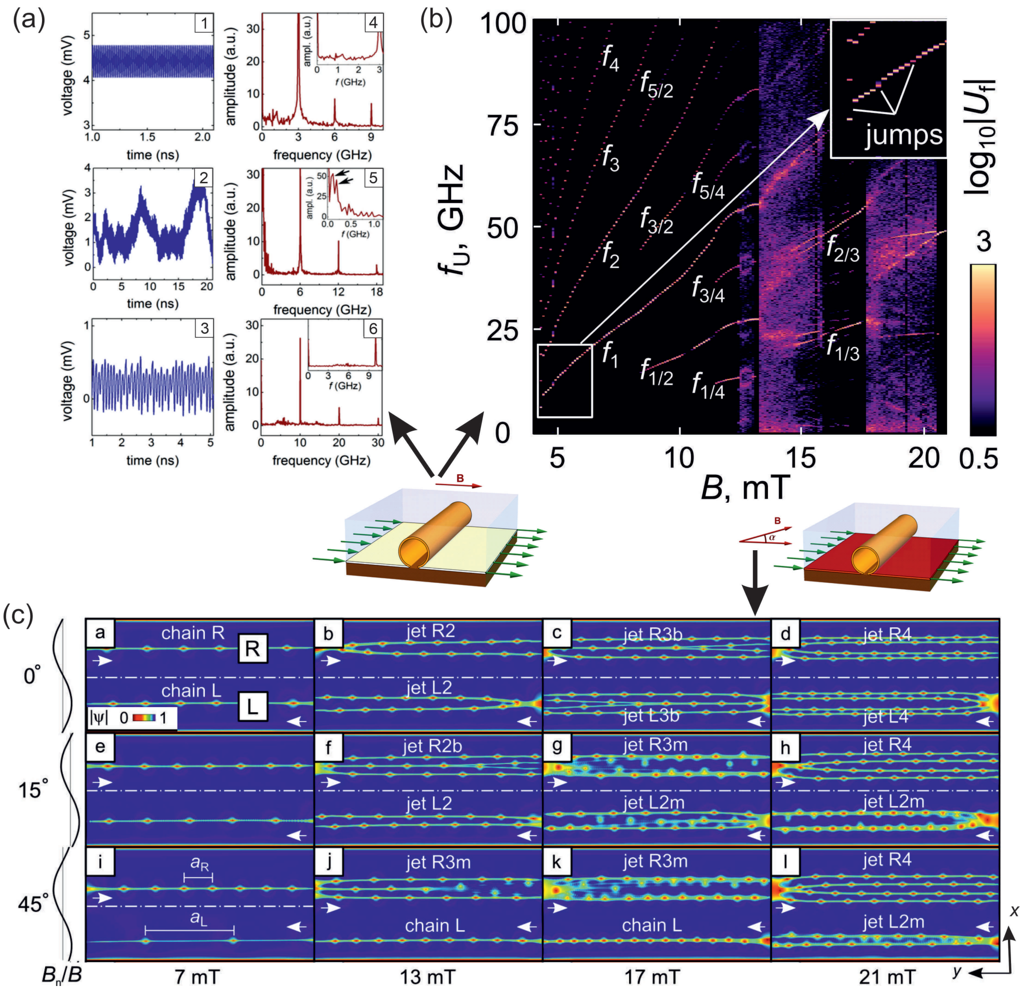

FIG. 3. Computationally unveiled geometry-driven topological phenomena. (a) Effect of the ac frequency on the dynamics of topological defects in open Nb superconductor nanotubes. Adapted with permission[51]. Copyright 2022, Springer Nature. The time-dependent voltage (panels 1 to 3) and its FFT spectra (panels 4 to 6) at the magnetic field $B = 2$ mT, the dc transport current $j_0 = 2.1$ GAm^2 and the transport current modulation depth $j_1/j_0 = 0.5$ for the ac frequencies 3, 6, and 10 GHz. The second- and third-highest peaks are indicated by arrows in the inset of panel (5). (b) The frequency spectrum $f_U(B)$ as a function of the magnetic induction B for the nanotube with $R = 390$ nm at the transport current densities 16 GA/m^2 and 20 GA/m^2. Adapted with permission[52]. Copyright 2024, American Physical Society. (c) Snapshots of the absolute value of the superconducting order parameter $|\psi|$ overlaid with the accumulated vortex paths for the nanotube with $R = 390$ nm at the transport current density $j_{tr} = 16$ GA/m^2 under tiled magnetic fields. L: left; R: right (half-tube); M: middle; b: bifurcations; m: multifurcations. The number in the jet name corresponds to the number of vortex chains in the jet. Direction of the vortex motion is indicated by the arrows. The dash-dotted lines are the midlines. Adapted with permission[55]. Copyright 2024, MDPI.

tection (Fig. 4(a)). At present, the direct application of other well-established characterization methods, such as SQUID for superconductors at the microscale, has not yet demonstrated its suitability for 3D curved superconductors at the nanoscale.

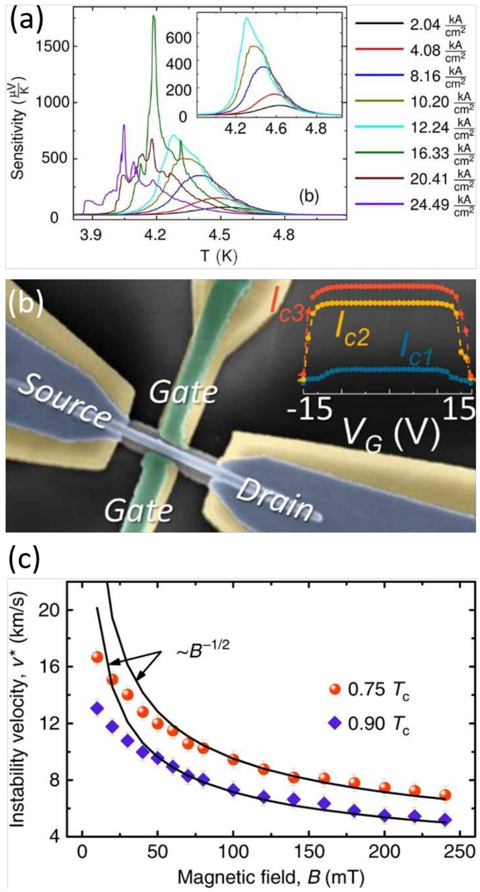

FIG. 4. (a) Sensitivity vs temperature (inset: details for low-current densities) for a rolled-up Nb nanohelix. Reproduced with permission[22]. Copyright 2019, American Chemical Society. (b) Geometry of a suspended Ti gated superconductor transistor. Inset: switching currents I_{C1}, I_{C2}, I_{C3} as a function of V_G measured at very low bath temperatures. Reproduced with permission[59]. Copyright 2020, American Chemical Society. (c) The instability velocity v^* as a function of the magnetic field in Nb-C microwires grown with Ga$^+$ FIBID. Reproduced with permission[65]. Copyright 2020, Springer Nature.

Consequently, there is an urgent need to advance the adaptation of microscale techniques or propose original approaches to facilitate the comprehensive characterization of 3D superconducting nanoarchitectures..

iii) Application design.

1. To enhance by orders of magnitude sensitivity of superconductor nanosensors of the magnetic field[53] and to design innovative superconductor quantum interference filters and switches based, e.g., on the controlled vortex dynamics and topological transition between vortex-chain- and phase-slip-regimes in superconductor open nanotubes and hybrid nanostructures[51].

2. To develop robust elements for fluxon-based quantum information processing and quantum computing, e. g., self-assembled networks of Josephson Junctions, parametric amplifiers, memory elements, superconducting qubits, and frequency generators, based on sustainable double fluxon transmission lines in superconductor open nanotubes [11].

3. To design superconductor nanostructured bolometers and THz-detectors, which provide a significant advancement in sensitivity and reduction in noise as compared to the available ones, e.g., using superconductor nanohelices [22].

4. To extend the fascinating topological properties of quantum fields, including unprecedented continuous control of the Berry phase, revealed recently in Möbius-stripe waveguides[5] onto superconductor Möbius-like nanoarchitectures.

B. in the computational and theoretical studies

1. To model and simulate the physical phenomena inherent in fabrication methods for the creation of 3D superconductor nanoarchitectures, which anticipate proximity and heating effects.

2. To expedite optimization and improve reproducibility in FIB processing using Deep Learning, which may be deployed in near-real time[71].

3. To explore the physics of superconducting fluctuations, in particular, to unveil the effects of fluctuations of the order parameter on properties of 3D nanoarchitectures above T_c [72]. To understand the role of correlated disorder and ordered impurities in superconductor 3D nanoarchitectures towards targeted design of their functional properties for responsive media, thermoelectrics and topological phases[73]. To analyze edge defects, which determine vortex (de)nucleation in superconductor 3D nanoarchitectures.

4. To investigate the impact of confinement of superconductors into 3D nanoarchitectures on the amplitude (or Higgs) mode of the order-parameter fluctuation through the nonlinear light-Higgs coupling[74,75].

5. To incorporate the (dc+ac)-driven escape of quasiparticles from the vortex cores, leading to the complex dynamics of vortices surrounded by a cloud of quasiparticles (the flux-flow instability) in superconductor 3D nanoarchitectures[76].

6. To study the interplay between superconductivity and chirality or noncentrosymmetry aimed at prediction of nonreciprocical transport effects in superconductor 3D nanoarchitectures.
7. To develop efficient high-performance methods for the numerical simulations of superconductor 3D nanoarchitectures of complicated geometry, like the algorithm based on the differential-geometry formalism [77].

In conclusion, our manuscript presents a comprehensive overview of recent advancements in the fabrication and characterization of 3D nano-superconductors with unconventional topologies of superconducting states. We have highlighted the significant challenges faced in experimental work in this field and emphasized the importance of overcoming these obstacles to unlock the full potential of these materials for various technological applications. By elucidating the fascinating physical properties arising from geometry-induced topology and chirality, our work aims to catalyze further research in this area and contribute to the front-line development of modern technologies. We believe that it will serve as a valuable resource for researchers and engineers working in the field of applied physics and nanotechnologies.

ACKNOWLEDGMENTS

This article is based upon work supported by the Generalitat Valenciana (SEJIGENT/2021/012T), the Grant RYC2020-029075-I funded by MCIN/AEI/ 10.13039/501100011033 and by "ESF Investing in your future" and the European Cooperation in Science and Technology COST Actions CA21144 (SuperQuMap) and CA16218 (FIT4NANo). The authors are grateful to numerous current and former collaborators on the present topic over the past years: J. M. De Teresa, I. Guillamón, D. Mailly, P. Orús, R. O. Rezaev, O. G. Schmidt, E. I. Smirnova, H. Suderow, and U. Zeitler. R.C. thanks A. Arroyo-Fructuoso, G. Hlawacek, and A. Ibarra. V.M.F. thanks I. A. Bogush, M. D. Croitoru, V. N. Gladilin, D. Grimm, O. V. Dobrovolskiy, and R. Wördenweber.

DATA AVAILABILITY

Data sharing is not applicable to this article as no new data were created or analyzed in this study.

[1] Helmut Eschrig, "Introduction," in *Topology and Geometry for Physics* (Springer Berlin Heidelberg, Berlin, Heidelberg, 2011) p. 390.

[2] Georges H. Wagnière, in *On Chirality and the Universal Asymmetry. Reflections on Image and Mirror Image* (Verlag Helvetica Chimica Acta, Zürich, 2007) p. 247.

[3] V. M. Fomin, *Topology-driven effects in advanced nanoarchitectures, in* A. Sidorenko (Ed.), *Functional Nanostructures and Metamaterials for Superconducting Spintronics. From Superconducting Qubits to Self-Organized Nanostructures* (Springer International Publishing, Cham, 2018) pp. 195 – 220.

[4] Benjamin J. Wieder, Barry Bradlyn, Jennifer Cano, Zhijun Wang, Maia G. Vergniory, Luis Elcoro, Alexey A. Soluyanov, Claudia Felser, Titus Neupert, Nicolas Regnault, and B. Andrei Bernevig, "Topological materials discovery from crystal symmetry," Nature Reviews Materials **7**, 196 (2022).

[5] Jiawei Wang, Sreeramulu Valligatla, Yin Yin, Lukas Schwarz, Mariana Medina-Sanchez, Stefan Baunack, Ching Hua Lee, Ronny Thomale, Shilong Li, Vladimir M. Fomin, Libo Ma, and Oliver G. Schmidt, "Experimental observation of berry phases in optical möbius-strip microcavities," Nature Photonics **17**, 120–125 (2023).

[6] O. Volkov, O. Pylypovskyi, F. Porrati, F. Kronast, J. A. Fernandez Roldan, A. Kakay, A. Kuprava, S. Barth, F. N. Rybakov, O. Eriksson, S. Lamb-Camarena, P. Makushko, M.-A. Mawass, S. Shakeel, O. V. Dobrovolskiy, M. Huth, and D. Makarov, "Three-dimensional magnetic nanotextures with high-order vorticity in soft magnetic wireframes," Nature Communications **15**, 2193 (2024).

[7] V. M. Fomin, *Self-Rolled Micro- and Nanoarchitectures: Effects of Topology and Geometry* (De Gruyter, Berlin–Boston, 2021).

[8] J. Tempere, V. N. Gladilin, I. F. Silvera, J. T. Devreese, and V. V. Moshchalkov, "Coexistence of the meissner and vortex states on a nanoscale superconducting spherical shell," Phys. Rev. B **79**, 134516 (2009).

[9] P. Sabatino, G. Carapella, and G. Costabile, "Magneto-transport properties of curved mesoscopic superconducting strips," Supercond. Sci. Technol. **24**, 125007 (2011).

[10] V. N. Gladilin, J. Tempere, J. T. Devreese, and V. V. Moshchalkov, "Aharonov-bohm oscillations in the vortex dynamics in superconducting hollow cylinders," Phys. Rev. B **86**, 104508 (2012).

[11] Vladimir M. Fomin, Roman O. Rezaev, and Oliver G. Schmidt, "Tunable Generation of Correlated Vortices in Open Superconductor Tubes," Nano Letters **12**, 1282–1287 (2012).

[12] R.O. Rezaev, V.M. Fomin, and O.G. Schmidt, "Vortex dynamics controlled by pinning centers on Nb superconductor open microtubes," Physica C: Superconductivity and its Applications **497**, 1–5 (2014).

[13] Vladimir M Fomin, Roman O Rezaev, Evgenii A Levchenko, Daniel Grimm, and Oliver G Schmidt, "Superconducting properties of nanostructured microhelices," Journal of Physics: Condensed Matter **29**, 395301 (2017).

[14] Denys Makarov, Oleksii M. Volkov, Attila Kákay, Oleksandr V. Pylypovskyi, Barbora Budinská, and Oleksandr V. Dobrovolskiy, "New Dimension in Magnetism and Superconductivity: 3D and Curvilinear Nanoarchitectures," Advanced Materials **34**, 2101758 (2022).

[15] Paola Gentile, Mario Cuoco, Oleksii M. Volkov, Zu-Jian Ying, Ivan J. Vera-Marun, Denys Makarov, and Carmine Ortix, "Electronic materials with nanoscale curved geometries," Nature Electronics **5** (2022), 10.1038/s41928-022-00820-z.

[16] Andrea Tononi and Luca Salasnich, "Low-dimensional quantum gases in curved geometries," Nature Reviews Physics 2023 5:7 **5**, 398–406 (2023).

[17] F. Qin, W. Shi, T. Ideue, M. Yoshida, A. Zak, R. Tenne, T. Kikitsu, D. Inoue, D. Hashizume, and Y. Iwasa, "Superconductivity in a chiral nanotube," Nature Communications **8**, 1–6 (2017).

[18] V.Ya Prinz, V. A. Seleznev, A. K. Gutakovsky, A. V. Chehovskiy, V. V. Preobrazhenskii, M. A. Putyato, and T. A. Gavrilova, "Free-standing and overgrown InGaAs/GaAs nanotubes, nanohelices and their arrays," Physica E **6**, 828–831 (2000).

[19] O. G. Schmidt and K. Eberl, "Thin solid films roll up into nanotubes," Nature **410**, 168–168 (2001).

[20] D. J. Thurmer, C. Deneke, and O. G. Schmidt, "In situ monitoring of the complex rolling behaviour of InGaAs/GaAs/Nb hybrid microtubes," J. Phys. D **41**, 205419 (2008).

[21] D. J. Thurmer, C. C. B. Bufon, Ch. Deneke, and O. G. Schmidt, "Nanomembrane-based mesoscopic superconducting hybrid junctions," Nano Lett. **10**, 3704–3709 (2010).

[22] Sören Lösch, Alexey Alfonsov, Oleksandr V. Dobrovolskiy, Robert Keil, Vivienne Engemaier, Stefan Baunack, Guodong Li, Oliver G. Schmidt, and Danilo Bürger, "Microwave radiation detection with an ultrathin free-standing superconducting niobium nanohelix," ACS Nano **13**, 2948–2955 (2019).

[23] G. J. Dolan, "Offset masks for lift-off photoprocessing," Applied Physics Letters **31**, 337–339 (1977).

[24] Ivan V. Pechenezhskiy, Raymond A. Mencia, Long B. Nguyen, Yen-Hsiang Lin, and Vladimir E. Manucharyan, "The superconducting quasicharge qubit," Nature **585**, 368–371 (2020).

[25] Lior Shani, Aaron N. Michelson, Brian Minevich, Yafit Fleger, Michael Stern, Avner Shaulov, Yosef Yeshurun, and Oleg Gang, "DNA-assembled superconducting 3D nanoscale architectures," Nature Communications **11**, 5697 (2020).

[26] Rosa Córdoba, "Additive nanofabrication using focused ion and electron beams," in *Encyclopedia of Condensed Matter Physics* (Elsevier, 2024) pp. 448–464.

[27] Pablo Orús, Fabian Sigloch, Soraya Sangiao, and José María De Teresa, "Superconducting materials and devices grown by focused ion and electron beam induced deposition," Nanomaterials **12** (2022), 10.3390/nano12081367.

[28] Wuxia Li, Changzhi Gu, and P A Warburton, "Superconductivity of Freestanding Tungsten Nanofeatures Grown by Focused-Ion-Beam," Journal of Nanoscience and Nanotechnology **10**, 7436–7438 (2010).

[29] E. J. Romans, E. J. Osley, L. Young, P. A. Warburton, and W. Li, "Three-dimensional nanoscale superconducting quantum interference device pickup loops," Applied Physics Letters **97**, 222506 (2010).

[30] Wuxia Li, J C Fenton, Ajuan Cui, Huan Wang, Yiqian Wang, Changzhi Gu, D W McComb, and P A Warburton, "Felling of individual freestanding nanoobjects using focused-ion-beam milling for investigations of structural and transport properties," Nanotechnology **23**, 105301 (2012).

[31] Fabrizio Porrati, Sven Barth, Roland Sachser, Oleksandr V. Dobrovolskiy, Anja Seybert, Achilleas S. Frangakis, and Michael Huth, "Crystalline Niobium Carbide Superconducting Nanowires Prepared by Focused Ion Beam Direct Writing," ACS Nano **13**, acsnano.9b00059 (2019).

[32] Pablo Orús, Fabian Sigloch, Soraya Sangiao, and José María De Teresa, "Superconducting w-c nanopillars fabricated by ga+ focused ion beam induced deposition," Journal of Solid State Chemistry **315**, 123476 (2022).

[33] Rosa Córdoba, Alfonso Ibarra, Dominique Mailly, and José Ma De Teresa, "Vertical Growth of Superconducting Crystalline Hollow Nanowires by He + Focused Ion Beam Induced Deposition," Nano Letters **18**, 1379–1386 (2018).

[34] Rosa Córdoba, Alfonso Ibarra, Dominique Mailly, Isabel Guillamón, Hermann Suderow, and José María De Teresa, "3D superconducting hollow nanowires with tailored diameters grown by focused He + beam direct writing," Beilstein Journal of Nanotechnology **11**, 1198–1206 (2020).

[35] Rosa Córdoba, Dominique Mailly, Roman O. Rezaev, Ekaterina I. Smirnova, Oliver G. Schmidt, Vladimir M. Fomin, Uli Zeitler, Isabel Guillamón, Hermann Suderow, and José María De Teresa, "Three-Dimensional Superconducting Nanohelices Grown by He + -Focused-Ion-Beam Direct Writing," Nano Letters **19**, 8597–8604 (2019).

[36] Katja Höflich, Gerhard Hobler, Frances I. Allen, Tom Wirtz, Gemma Rius, Lisa McElwee-White, Arkady V. Krasheninnikov, Matthias Schmidt, Ivo Utke, Nico Klingner, Markus Osenberg, Rosa Córdoba, Flyura Djurabekova, Ingo Manke, Philip Moll, Mariachiara Manoccio, José Marıa De Teresa, Lothar Bischoff, Johann Michler, Olivier De Castro, Anne Delobbe, Peter Dunne, Oleksandr V. Dobrovolskiy, Natalie Frese, Armin Gölzhäuser, Paul Mazarov, Dieter Koelle, Wolfhard Möller, Francesc Pérez-Murano, Patrick Philipp, Florian Vollnhals, and Gregor Hlawacek, "Roadmap for focused ion beam technologies," Applied Physics Reviews **10** (2023), 10.1063/5.0162597, arXiv:2305.19631.

[37] Gediminas Seniutinas, Armandas Balčytis, Ignas Reklaitis, Feng Chen, Jeffrey Davis, Christian David, and Saulius Juodkazis, "Tipping solutions: emerging 3D nano-fabrication/ -imaging technologies," Nanophotonics **6**, 385307 (2017).

[38] Sebastian Bochmann, Dirk Döhler, Beatrix Trapp, Michal Staňo, Olivier Fruchart, and Julien Bachmann, "Preparation and physical properties of soft magnetic nickel-cobalt three-segmented nanowires," Journal of Applied Physics **124**, 163907 (2018).

[39] Luca Hirt, Alain Reiser, Ralph Spolenak, and Tomaso Zambelli, "Additive Manufacturing of Metal Structures at the Micrometer Scale," Advanced Materials **29**, 1604211 (2017).

[40] Larry Scipioni, Lewis Stern, and John Notte, "Applications of the helium ion microscope," Microscopy Today **15**, 12–15 (2007).

[41] Diederik Maas, Emile van Veldhoven, Ping Chen, Vadim Sidorkin, Huub Salemink, Emile .. van der Drift, and Paul Alkemade, "Nanofabrication with a helium ion microscope," in *Metrology, Inspection, and Process Control for Microlithography Xxiv*, Vol. 7638, edited by Christopher J Raymond (SPIE, 2010) p. 763814.

[42] Shamashis Sengupta, Chuan Li, Cedric Baumier, Alik Kasumov, S. Guéron, H. Bouchiat, and F. Fortuna, "Superconducting nanowires by electron-beam-induced deposition," Applied Physics Letters **106**, 042601 (2015).

[43] Tycho J. Blom, Thomas W. Mechielsen, Remko Fermin, Marcel B.S. Hesselberth, Jan Aarts, and Kaveh Lahabi, "Direct-Write Printing of Josephson Junctions in a Scanning Electron Microscope," ACS Nano **15**, 322–329 (2021).

[44] M. Winhold, P. M. Weirich, C. H. Schwalb, and M. Huth, "Superconductivity and metallic behavior in PbxCyOδ structures prepared by focused electron beam induced deposition," Applied Physics Letters **105**, 162603 (2014).

[45] Kazumasa Makise, Kazutaka Mitsuishi, Masayuki Shimojo, and Bunju Shinozaki, "Microstructural analysis and transport properties of MoO and MoC nanostructures prepared by focused electron beam-induced deposition," Scientific Reports **4**, 5740 (2014).

[46] Victor Deinhart, Lisa-Marie Kern, Jan N Kirchhof, Sabrina Juergensen, Joris Sturm, Enno Krauss, Thorsten Feichtner, Sviatoslav Kovalchuk, Michael Schneider, Dieter Engel, Bastian Pfau, Bert Hecht, Kirill I Bolotin, Stephanie Reich, and Katja Höflich, "The patterning toolbox FIB-o-mat: Exploiting the full potential of focused helium ions for nanofabrication," Beilstein Journal of Nanotechnology **12**, 304–318 (2021).

[47] Jason D. Fowlkes, Robert Winkler, Brett B. Lewis, Michael G. Stanford, Harald Plank, and Philip D. Rack, "Simulation-Guided 3D Nanomanufacturing via Focused Electron Beam Induced Deposition," ACS Nano **10**, 6163–6172 (2016).

[48] Luka Skoric, Dédalo Sanz-Hernández, Fanfan Meng, Claire Donnelly, Sara Merino-Aceituno, and Amalio Fernández-Pacheco, "Layer-by-Layer Growth of Complex-Shaped Three-Dimensional Nanostructures with Focused Electron Beams," Nano Letters **20**, 184–191 (2020).

[49] Lukas Keller and Michael Huth, "Pattern generation for direct-write three-dimensional nanoscale structures via focused electron beam induced deposition," Beilstein Journal of Nanotechnology **9**, 2581–2598 (2018).

[50] Rosa Córdoba, T I Baturina, J Sesé, A Yu Mironov, J M De Teresa, M. R. Ibarra, D. A. Nasimov, A. K. Gutakovskii, A. V. Latyshev, I. Guillamón, H. Suderow, S. Vieira, M. R. Baklanov, J. J. Palacios, and V. M. Vinokur, English"Magnetic field-induced dissipation-free state in superconducting nanostructures." Nature communications **4**, 1437 (2013).

[51] V. M. Fomin, R. O. Rezaev, and O. V. Dobrovolskiy, "Topological transitions in ac/dc-driven superconductor nanotubes," Sci. Rep. **12**, 10069 (2022).

[52] Igor Bogush, Oleksandr V. Dobrovolskiy, and Vladimir M. Fomin, "Microwave generation and vortex jets in superconductor nanotubes," Phys. Rev. B **109**, 104516 (2024).

[53] V. M. Fomin, R. O. Rezaev, E. I. Smirnova, and O. G. Schmidt, "Topological transitions in superconductor nanomembranes in a magnetic field with submicron inhomogeneity under a strong transport current," Comm. Phys. **3**, 144 (2020).

[54] I. Bogush and V. M. Fomin, "Topological defects in open superconducting nanotubes after gradual and abrupt switching of the transport current and magnetic field," Phys. Rev. B **105**, 094511 (2022).

[55] I. Bogusch, V. M. Fomin, and O. V. Dobrovolskiy, "Steering of vortices by magnetic field tilting in open superconductor nanotubes," Nanomaterials **14**, 420 (2024).

[56] Lei Chen, Lili Wu, Yue Wang, Yinping Pan, Denghui Zhang, Junwen Zeng, Xiaoyu Liu, Linxian Ma, Wei Peng, Yihua Wang, Jie Ren, and Zhen Wang, "Miniaturization of the Superconducting Memory Cell via a Three-Dimensional Nb Nano-superconducting Quantum Interference Device," ACS Nano **14**, 11002–11008 (2020).

[57] Gaia Germanese, Federico Paolucci, Giampiero Marchegiani, Alessandro Braggio, and Francesco Giazotto, "Bipolar thermoelectric Josephson engine," Nature Nanotechnology **17**, 1084–1090 (2022).

[58] Muhammad Fahlesa Fatahilah, Klaas Strempel, Feng Yu, Sindhuri Vodapally, Andreas Waag, and Hutomo Suryo Wasisto, "3D GaN nanoarchitecture for field-effect transistors," Micro and Nano Engineering **3**, 59–81 (2019).

[59] Mirko Rocci, Giorgio De Simoni, Claudio Puglia, Davide Degli Esposti, Elia Strambini, Valentina Zannier, Lucia Sorba, and Francesco Giazotto, "Gate-Controlled Suspended Titanium Nanobridge Supercurrent Transistor," ACS Nano **14**, 12621–12628 (2020).

[60] Pablo Orús, Vladimir M. Fomin, José María De Teresa, and Rosa Córdoba, "Critical current modulation induced by an electric field in superconducting tungsten-carbon nanowires," Scientific Reports **11**, 17698 (2021).

[61] C. Puglia, G. De Simoni, and F. Giazotto, "Electrostatic Control of Phase Slips in Ti Josephson Nanotransistors," Physical Review Applied **13**, 054026 (2020).

[62] Denis Vasyukov, Yonathan Anahory, Lior Embon, Dorri Halbertal, Jo Cuppens, Lior Neeman, Amit Finkler, Yehonathan Segev, Yuri Myasoedov, Michael L. Rappaport, Martin E. Huber, and Eli Zeldov, "A scanning superconducting quantum interference device with single electron spin sensitivity," Nature Nanotechnology **8**, 639–644 (2013).

[63] Y. Anahory, H. R. Naren, E. O. Lachman, S. Buhbut Sinai, A. Uri, L. Embon, E. Yaakobi, Y. Myasoedov, M. E. Huber, R. Klajn, and E. Zeldov, "SQUID-on-tip with single-electron spin sensitivity for high-field and ultra-low temperature nanomagnetic imaging," Nanoscale **12**, 3174–3182 (2020).

[64] L. Ceccarelli, D. Vasyukov, M. Wyss, G. Romagnoli, N. Rossi, L. Moser, and M. Poggio, "Imaging pinning and expulsion of individual superconducting vortices in amorphous mosi thin films," Phys. Rev. B **100**, 104504 (2019).

[65] O. V. Dobrovolskiy, D. Yu Vodolazov, F. Porrati, R. Sachser, V. M. Bevz, M. Yu Mikhailov, A. V. Chumak, and M. Huth, "Ultrafast vortex motion in a direct-write Nb-C superconductor," Nature Communications **11**, 3291 (2020).

[66] "Vladimir M. Fomin, Superconductivity in self-rolled nanoarchitectures," Research Features **138**, 98–101 (2021).

[67] V. M. Fomin and O. V. Dobrovolskiy, "A perspective on superconductivity in curved 3D nanoarchitectures," Appl. Phys. Lett. **120**, 090501 (2022).

[68] Satoshi Tanda, Taku Tsuneta, Yoshitoshi Okajima, Katsuhiko Inagaki, Kazuhiko Yamaya, and Noriyuki Hatakenaka, "A möbius strip of single crystals," Nature **397**, 398–417 (2002).

[69] Michael T. Taschuk, Matthew M. Hawkeye, and Michael J. Brett, "Chapter 13 - glancing angle deposition," in *Handbook of Deposition Technologies for Films and Coatings (Third Edition)*, edited by Peter M. Martin (William Andrew Publishing, Boston, 2010) third edition ed., pp. 621–678.

[70] Daniel Fu, Raghu Pradeep Narayanan, Abhay Prasad, Fei Zhang, Dewight Williams, John S. Schreck, Hao Yan, and John Reif, "Automated design of 3d dna origami with non-rasterized 2d curvature," Science Advances **8**, eade4455 (2022).

[71] Oleksandr Buchnev, James A. Grant-Jacob, Robert W. Eason, Nikolay I. Zheludev, Ben Mills, and Kevin F. MacDonald, "Deep-learning-assisted focused ion beam nanofabrication," Nano Letters **22**, 2734–2739 (2022).

[72] W. J. Skocpol and M. M Tinkham, "Fluctuations near superconducting phase transitions," Rep. Prog. Phys. **38**, 1049 (1975).

[73] Andrew L. Simonov, Arkadiy AU Goodwin, "Designing disorder into crystalline materials," Nature Reviews Chemistry **4**, 657–673 (2020).

[74] Ryo Shimano and Naoto Tsuji, "Higgs mode in superconductors," Annual Review of Condensed Matter Physics **11**, 103–124 (2020).

[75] L. Schwarz, B. Fauseweh, N. Tsuji, N. Cheng, N. Bittner, H. Krull, M. Berciu, G. S. Uhrig, A. P. Schnyder, S. Kaiser, and D. Manske, "Classification and characterization of nonequilibrium higgs modes in unconventional superconductors," Nature Communications **11**, 103–124 (2020).

[76] O.V. Dobrovolskiy, V.M. Bevz, E. Begun, R. Sachser, R.V. Vovk, and M. Huth, "Fast dynamics of guided magnetic flux quanta," Phys. Rev. Appl. **11**, 054064 (2019).

[77] I. Bogush and V. M. Fomin, "Reduction of the relativistic and non-relativistic GL models to a 2D curved surface," in *Nano-engineered Superconductors - NES21. Abstract book.* (Univerität Wien, 2022) p. 8.